American Journal of Water Science and Engineering
2021; 7(2): 39-47
http://www.sciencepublishinggroup.com/j/ajwse
doi: 10.11648/j.ajwse.20210702.12
ISSN: 2575-1867 (Print); ISSN: 2575-1875 (Online)

Effects of Plow-Tillage on Preventing and Controlling the Black Water Events in Shallow Lakes

He Yuhong[1, *], Zhou Qilin[2]

[1]Huatian Engineering & Technology Corporation, Metallurgical Corporation of China Ltd, Nanjing, China

[2]Nanjing Institute of Geography & Limnology, Chinese Academy of Sciences, Nanjing, China

Email address:
yuhongjiayou.hi@163.com (He Yuhong)

[*]Corresponding author

To cite this article:
He Yuhong, Zhou Qilin. Effects of Plow-Tillage on Preventing and Controlling the Black Water Events in Shallow Lakes. *American Journal of Water Science and Engineering*. Vol. 7, No. 2, 2021, pp. 39-47. doi: 10.11648/j.ajwse.20210702.12

Received: April 20, 2021; **Accepted**: May 7, 2021; **Published**: May 14, 2021

Abstract: The high organic loading sediment in the areas of algal accumulation are the primary cause of frequent occurrence of black water in the western Chao Lake. Through an algal accumulation experiment, plow-tillage based on resuspension characteristics and its effect on lake sediment was assessed using a large device capable of simulating lake-winds and sediment resuspension. The dynamics of overlying water coloration, ρ(Fe^{2+}), ρ(S2-) in the process of black water induction, the key physicochemical characteristics of newly formed water–sediment interface, and iron and sulfur variations in interstitial-water and their response to plow-tillage were examined. The results showed that plow-tillage depth significantly influenced black-water formation; a 15 cm plow-tillage depth helped in controlling black-water. When black water occurred in other plow-tillage controls, i.e., (2, 5, and 10 cm), along with blank-treatments during day 8 to 14, typical overlying water characteristics [ρ(Fe^{2+}) and ρ(S2-)] of the plow-tillage 15 cm treatments were 68.6%, 79.5%, 48.1%, 46.7%, and 51.3%; and 75.2%, 65.7%, 57.1%, 74.5%, and 75.0%, respectively, in comparison to that of the other plow-tillage controls and blank-treatments. Further analysis of the bottom-water and bottom-sediments revealed that the 15 cm plow-tillage depth treatment significantly enhanced the tolerance of the fresh water–sediment interface to algal accumulation and anoxic environments. Through the black water induction simulation, the dissolved oxygen concentration, redox potential, and pH of the bottom-water and at the interface were observably much higher than those in the black-water groups. However, ρ(ΣH_2S) was significantly lower than that of other treatments. The ρ(Fe^{2+}) in the surface-sediment water was 0.54 mg/L, which corresponds only 25.3–33.7% that of the black-water groups. Fe^{2+} accounted for 25.2% of the total iron, being considerably lower than ~40.0% of the black-water groups. The concentration of acid-volatile sulfides was 0.51 μg/g, which corresponds only 14.6–17.2% that of the black-water groups. Overall, plow-tillage helped to physically improve sediment in areas of algal accumulation. Plow-tillage could help turn surface-sediment overloaded with organic pollutants to the lower-layer, blocking material migration and supply of contaminated surface-sediment, and controlling anaerobic microbial activity. It could prevent the formation of black water-generating substances in the water column where algae accumulate and die, effectively preventing the occurrence of black water.

Keywords: Plow-tillage, Shallow-lake, Algal Accumulation, Black-water Events

1. Introduction

The turbid-green color of overlying water induced by excessive phytoplankton blooms is characteristic of eutrophic water-bodies [1]; however, a continuous decline of dissolved oxygen (DO) in the overlying water could lead to even serious ecological problems [2]. Residues of aquatic plants and algae descend to the bottom, enabling organic-matter circulation and accelerated respiration of microorganisms, causing concentration of dissolved oxygen [ρ(DO)] to continuously decline [3, 4]. Along with the formation of hypoxic, anoxic, or even anaerobic conditions in overlying water and sediments, the black-water phenomenon is induced by an interaction among residues of macrophytes, algae, and sediments;

typically characterized by black coloration, fetidness, and water turbidity [5-7]. In recent years, the black-water phenomenon occurred occasionally in severely eutrophic areas, e.g., Western Taihu Lake and Chaohu Lake. In 2007, the drinking water crisis near South Spring Waterworks caused by black water made the government and research community pay more attention in preventing and controlling black water.

The studies that investigated the Taihu Lake found that black-water events mainly occurred in areas with thick silt flow on the sediment surface, where algae accumulated easily [8]. It has been proved that black water cannot occur only by algal accumulation, but also by polluted sediments [9]. Subsequently, reduction products of Fe^{2+} and S accumulate in quantity, which eventually provide material support to generate black matter. Consequently, in algal accumulation areas, surface-treatments of contaminated sediments targeted at changing the vertical distribution of key blackening agents, could prevent and control formation of black water effectively [10]. Dredging projects in Yueliang Bay of Taihu Lake, South Spring Waterworks, and Fudu Harbor helped in controlling the formation and severity of black water [11]. Previous studies implemented plow-tillage (PT) to reconstruct tidal flats for breeding [12-13] and improve the sediment quality of lakes [14] and seas [15].

PT is a relatively cost-effective and non-invasive technique for sediment remediation by relocating polluted surface-sediment to greater depths. We believe that our study is the first to introduce PT as a method of controlling black water in aquatic ecosystems. An induced black-water phenomenon was simulated at different PT-depths in a laboratory to explore the relationship between PT-depth and black-water events in algal accumulation areas, and to discuss the feasibility of the former in controlling the latter.

2. Materials and Methods

2.1. Study Area and Sampling

Sediments and overlying water samples were obtained from the northwestern Chaohu Lake near the estuary area of Nanfei River (31°41′44″N, 117°24′32″E), which was eutrophic and severely polluted due to incoming water from Nanfei River. Moreover, significant algal blooms have been occurring annually with an increasing frequency and intensity in recent decades, and the western Chaohu Lake is considered to be black-water area.

Sediment cores with overlying water and an undisturbed sediment–water interface were collected using a gravity core sampler (Rigo Co. Ltd., Ø110 mm×L500 mm, Japan). Additionally, a cyanobacterial sample was collected by sieving lake surface-water through a 50-mm plankton net and then preserved at 4°C.

2.2. Experimental Design

A PT-depth of 2 cm was set to simulate the turbulent, resuspended, and redepositional conditions of algae accumulating sediments, as the sampling-site was severely disturbed by human activity and its bank was eroded by southeasterly winds. Varying PT-depths were employed by mixing the filtered cyanobacteria with various thicknesses of surface-sediments.

Treatment “Blank” was set as the original sediment core without PT and cyanobacteria, whereas treatment “CK” was set by adding 10 g of cyanobacteria, but without PT. Four PT-depths were considered: 2 cm (PT2), 5 cm (PT5), 10 cm (PT10), and 15 cm (PT15). Approximately 10 g of filtered cyanobacteria were homogenized with the plowed surface-sediment for each treatment. Subsequently, filtered lake water was gently injected to prevent disturbance at the interface. Each of the six treatments had three duplicated columns.

2.3. Experimental Induction of Black-Water Events

PT was simulated at day 60, at which time black-water events usually occur. The Unisense Micro Profiling System (Unisense, Aarhus, Denmark), which includes a microsensor multimeter, micromanipulator, motor controller, and microsensor, was employed to analyze DO, pH, concentration of H_2S ($\sum H_2S$), and redox potential profiles across the sediment–water interface. Additionally, all micro-electrodes were fully-polarized before use.

The sediment cores, collected algae, and lake water were used to simulate water in a Y-style sediment resuspension generation apparatus. For every treatment, 47.5 g/column algae (fresh weight) were added to the overlying water; the overlying water-depth in a single column was 180 cm. The lab-temperature was stabilized at (29±1) °C, being the average temperature of Chaohu Lake in July. Accordingly, wind conditions under speeds of 3.2 m/s were simulated daily in the Y-style apparatus during 13:00–17:00, and the experimental setup was kept under natural light; not applying any external light-source.

Fifty milliliters of water samples were taken per day from the middle of the water-columns to test $\rho(Fe^{2+})$, $\rho(S^{2-})$. Sediment cores were extracted from the apparatus at the end of the simulation. Immediately afterwards, DO, Ph, ΣH_2S, and Eh micro profiles at the sediment–water interface were analyzed. Each sediment core was then sliced at intervals of (0–1, 1–2, 2–4, 4–6, 6–8, and 8-10) cm, and preserved in an N_2 atmosphere. Physicochemical characteristics of the sediments were analyzed immediately after slicing to avoid oxidation.

2.4. Sampling Analysis

2.4.1. Identification of Water Coloration

Studies have proved that the black-water phenomenon is typically characterized mainly by blackened water and fetidness. The boundary between the black water and the rest of the water was easily distinguishable. It was difficult to confirm if the black-water phenomena occurred due to the complexity and diversity of volatile sulfurous compounds like H_2S and DMTS, which could have imparted fetidness [5]. Color differences were used to define various black-water levels; they were classified into four levels, designated as 0, 1,

2, and 3, corresponding to colorless, gray, light-black, and deep-black, respectively [11, 16]. The color-classification was recorded by one person to prevent subjective differences.

2.4.2. Measurements of ρ(DO), Eh, ρ(ΣH2S), and pH at the Sediment–Water Interface

Using microsensors of the Unisense OX-50, Unisense pH-50, Unisense H_2S-50, and Unisense ORP-50, sediment cores were probed to acquire DO, pH, ΣH_2S and Eh profiles in measurement steps of 100μm, respectively.

2.4.3. Chemical Analysis

Concentrations of Fe^{2+} and S^{2-} in the water samples were measured using a Shimadzu UV-2550 spectrophotometer. Fe^{2+} was measured using the ferrozine spectrophotometry method [17], S^{2-} by the methylene blue spectrophotometric method [18], and Fe by the oxalic acid–ammonium oxalate method [19]. AVS (acid volatile sulfide) from the sediments was extracted by previously used methods [20-22].

2.5. Statistical Analysis

Data and results were plotted using Origin 8.5 (OriginLab, Northampton, MA, USA) and Sigmaplot 12.5 (Systat Software, Inc., San Jose, CA, USA). Statistical significance was determined by one-way analysis of variance (ANOVA), followed by Tukey's post hoc test using SPSS 19.0 software. The significance level was reported as $P < 0.05$.

3. Results and Discussion

3.1. Effects of PT on Black-water Characteristics

The black-water phenomena occurred across all treatments during the experiment, except for PT15. And the identifying indicator was the black-coloration of the water-columns. The water of Blank, CK, PT2, PT5, and PT10 treatments blackened at day 9–10, 8, 10–11, 10–12, and 12–14, respectively. The phenomenon lasted for 8–10, 11, 6–7, 5–6, and 5 days, respectively. With a greater PT-depth, the water coloration in PT10 was remarkably lighter (grey/light-black) than others (black). The phenomenon in the CK columns lasted for longer than in other sets, suggesting that dead cyanobacteria subsided to the sediment-surface, accelerating the black-water phenomena occurring frequently in algal accumulation areas.

3.2. Effects of PT on DO, Eh, pH, and ΣH₂S Distribution at the Sediment–Water Micro Interface

3.2.1. Dissolved Oxygen (DO)

DO is an important indicator of oxidation–reduction environments in lake water which can influence the biogeochemical cycles of nutrients, sulfides, and heavy metals [23]. DO penetration depths range from a few millimeters to centimeters for different sediment types [24-25].

Herein, DO penetration depths at the sediment–water interface were significantly different, before and after the black-water phenomena in all treatments. According to Figure 1, preceding the experiments, the DO penetration depths of the Blank, CK, PT2, PT5, PT10, and PT15 treatments were 6.6, 0, 8, 5.4, 13.4, and 6.6 mm respectively, which could be arrayed as PT10 > PT2 > PT15=Blank > PT5 > CK. ρ(DO) values at the sediment–water interface for the Blank, CK, PT2, PT5, PT10, and PT15 treatments were 2.79, 1.47, 4.62, 5.90, 2.43, and 2.61 mg/L, respectively, i.e., PT5 > PT2 > Blank > PT15 > PT10 > CK.

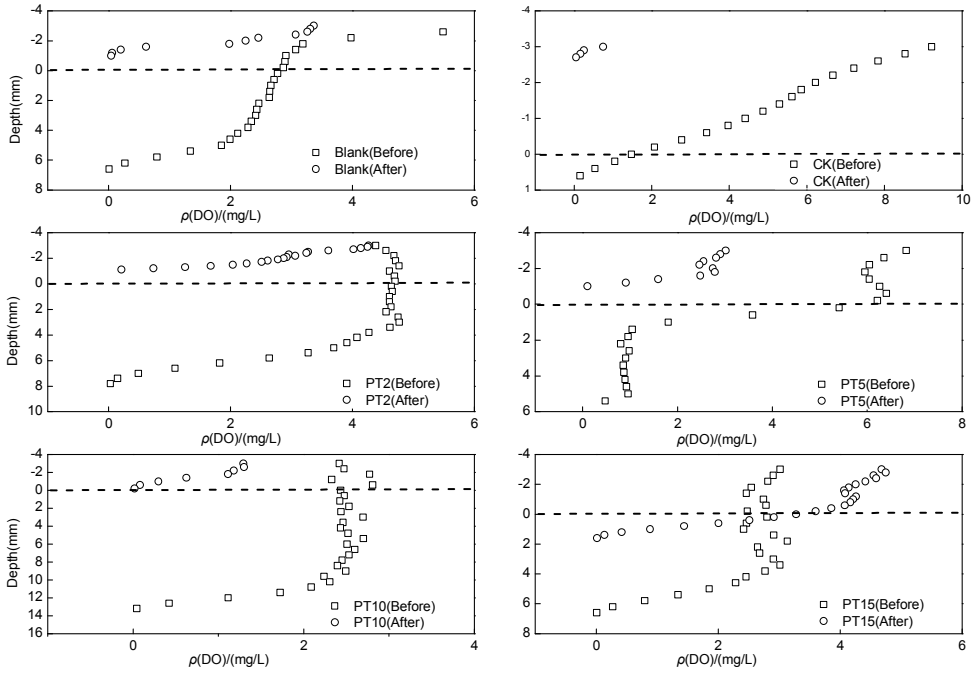

Figure 1. *DO profile of sediment-water interface before and after the black water events.*

Two aspects simultaneously led to an irregularity in both, the DO penetration depths, and ρ(DO) at the sediment–water interface of the PT treatments (P > 0.05): 1)With deeper PT, a greater amount of sediments below, rich in reductants was turned up to the sediment–water interface [26, 27]; 2) The cyanobacteria were mixed with the sediments and turned into the PT layer, reducing their amounts at the sediment–water interface, and increasing the DO concentration. For the CK treatments, both, ρ(DO) at the interface and DO penetration depths were the least among all groups (1.47 mg/L), and the water-columns were anoxic/anaerobic as the cyanobacteria decomposed in the overlying water and sediments, consuming the DO.

The DO concentration varied significantly along the longitudinal-profile of the sediments during the process, except for the "Blank" treatment. ρ(DO) was absent at the sediment–water interface of samples in which the black-water phenomena occurred, indicating that the formation and persistence of black water could lead to the overlying water and sediment–water interface becoming anerobic. For PT15, where the black-water phenomenon did not occur, ρ(DO) was observed at the sediment–water interface, and DO penetration depths decreased from 6.6 mm to 1.7 mm.

3.2.2. E_h

PT was implemented as a physical method for sediment remediation by relocating polluted surface-sediment to greater depths, forming a new sediment–water interface. According to Figure 2, the E_h distribution of all PT samples along the sediment longitudinal-profile tended towards that of the "Blank" treatment (as before the PT) [28], and it increased with an increasing PT-depth. At the relatively shallow PT-depths (PT2 and PT5), the polluted surface-sediment was only stirred, not overturned and buried. Moreover, a significant amount of dead cyanobacteria covered the surface-sediments and were decomposed by microorganisms, along with oxygen consumption, which also slowed down the recovery speed of E_h. E_h distribution along the sediment longitudinal-profile of "CK" was significantly lower than that of other treatments because of high cyanobacterial decomposition and no PT; its variation tendency was similar to that of the DO distribution along a longitudinal-profile.

As the sediments responded in varying degrees to the black-water phenomena, the variation tendency of E_h on the sediment surface differed accordingly. As presented in Figure 3, E_h at the sediment–water interface of PT15 (without black-water occurrence) was 123 mV, and decreased after the experiment, but the value still exceeded that of other PT samples, which were all <100 mV (P < 0.05). The variation in PT2 was insignificant, probably caused by existing anaerobic conditions before the simulation; also, the addition of cyanobacteria did not intensify the reduction reaction of the sediment. Based on the results of the PT treatments (PT2, PT5, PT10), E_h decreased with an increasing PT-depth.

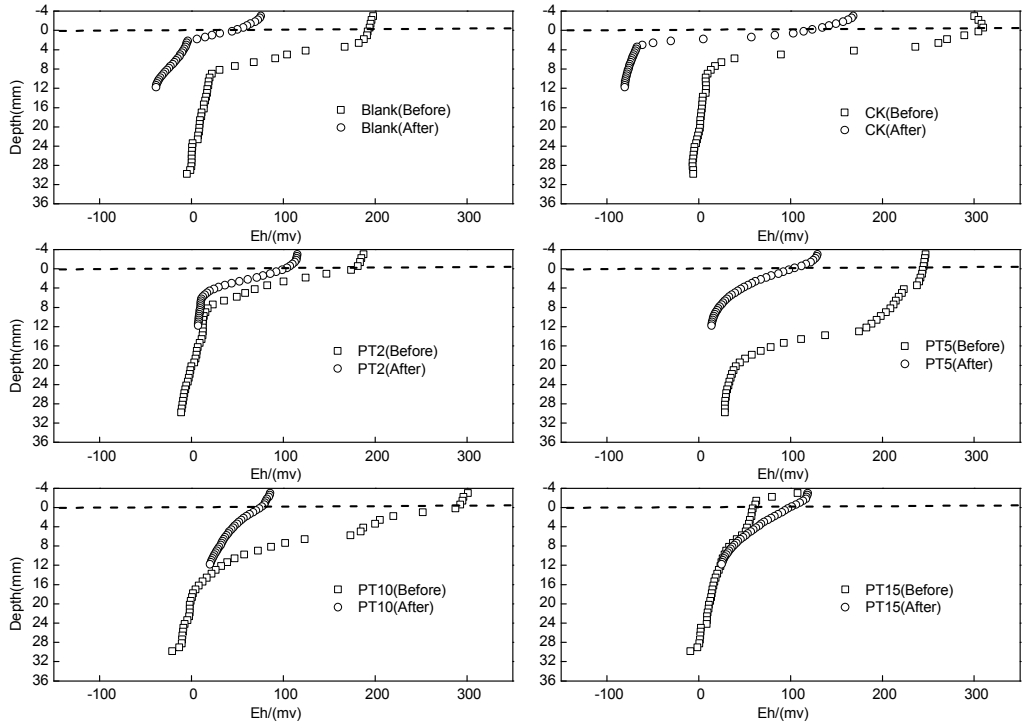

Figure 2. *E_h profile of sediment-water interface before and after the black water events.*

3.2.3. pH

At the bottom of an anoxic water-body, cyanobacteria-driven pH changes have a noticeable effect on sediment nutrient fluxes, causing nitrification–denitrification in a water-column [29], but the impact of pH variation on the black-water phenomena in bottom-water is still unclear.

According to Figure 3, PT influenced pH at the sediment–water interface insignificantly (P>0.05), while the addition of cyanobacteria made an apparent difference on pH (P<0.05). The pH at the sediment–water interface in all columns was elevated after the experiment, irrespective of the occurrence of black-water (P<0.05).

It has been demonstrated that an upward pH fluctuation can be buffered and controlled by acidic reduction through anaerobic reactions, cation exchanges (Ca^{2+}, Mg^{2+}) and reduction of sulfides [30]. Conversely, excess organic precipitation remains on the surface-sediment, beginning to ferment, and generates a significant amount of protons, which could cause pH to eventually decline [15]. Although, an excess amount of organic matter causing an increase in pH has been demonstrated for natural lakes [29]. Herein, an increasing pH was probably due to the deacidization of Fe and sulphates, and a reversal of the sulfate cycle, which could enable decomposition and consumption of accompanying protons [31]. The possible mechanism could be as follows: 1) In a relatively short time (about a week) natural sediments helped induce black-water formation; the duration was insufficient to produce sufficient fermentation and protons to cause a reversal of the sulfate cycle, enabling pH at the sediment–water interface to decline slightly; 2) Using dredged sediments, the quantity of sulfate reducing bacteria (SRB) in a column was insufficient [32], causing a lack of sufficient fermentation and protons, and resulting in a decreased pH; 3) Here, polluted sediment was plowed at varying depths, and pH in all treatments tended to increase. Following a reversal of the sulfate cycle, the reduced Fe and sulphates probably accepted most of the pre-existing protons over a relatively long duration (19 d), and constantly consumed newly generated ones, causing an eventual rise in pH.

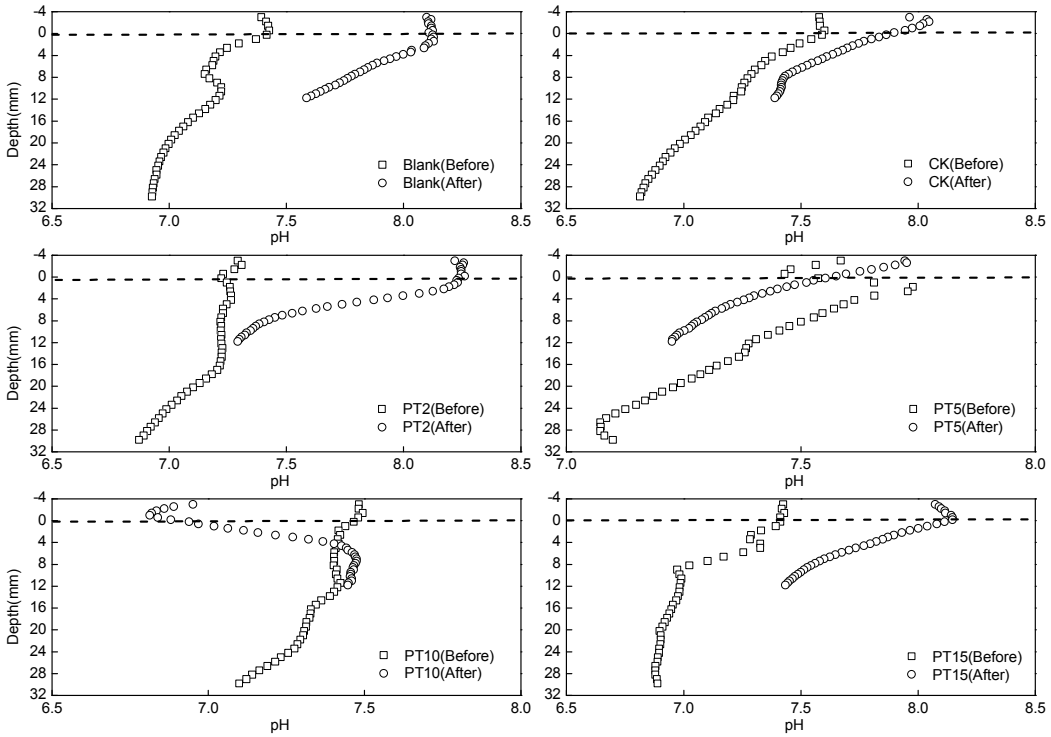

Figure 3. *pH profile of sediment-water interface before and after the black water events.*

3.2.4. ΣH_2S

Continuous anoxic conditions could result in redox conditions at the sediment–water interface and subject the chemical form of some sensitive elements, e.g., S, to redox conditions causing its transformation [23, 33]. Figure 4 shows the $\rho(\Sigma H_2S)$ changes at the sediment–water interface before and after the simulation. Before the simulation, trace ΣH_2S was detected at penetration depth of 0–12000μm among all treatments, suggesting that the sampled lake region was anoxic [34-36]. Moreover, ΣH_2S could be the material basis to form amorphous FeS, which could be considered as the main blackening agent [35]. Therefore, an understanding of ΣH_2S distribution in an aquatic ecosystem is critical for black-water management.

Abundant SRB and polluted sediment acted simultaneously to generate reducing sulfides, released to the overlying water in quantity; the process could be considered as the basis of the black-water phenomena [37]. $\rho(\Sigma H_2S)$ of both, the overlying surface-water and sediment interstitial-water in the treatments (Blank, CK, PT2, PT5, and PT10) increased markedly as compared to the values before the simulation ($P < 0.01$); also, greater the degree of black water (shown in Tab. 1), higher was the $\rho(\Sigma H_2S)$ in the sediment interstitial-water. Concurrently, a distinct ΣH_2S concentration difference was observed at the interface in the columns where black water formed. The ΣH_2S concentration was greater in the sediment than in overlying water, causing ΣH_2S to be diffused from the sediment and be gradually released into the overlying water.

In PT15, ΣH_2S concentration in the sediment interstitial-water (depth: 0–12 mm) changed insignificantly during the experiment ($P > 0.05$); there was no obvious gradient distribution at the interface, being different for other PT samples. However, $\rho(\Sigma H_2S)$ in the overlying water was higher than that in the sediment; probably because the algal residue contained sulfurous amino acid, providing "Sulfur".

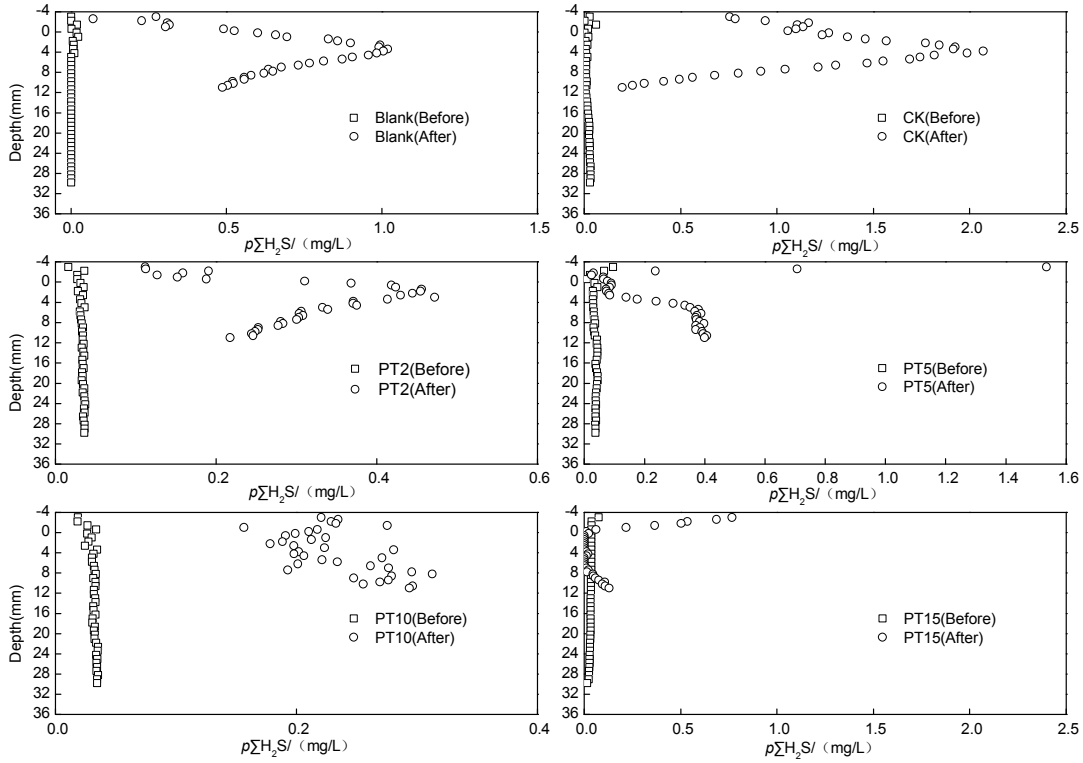

Figure 4. *H_2S profile of sediment-water interface before and after the black water events.*

3.3. Concentrations of Fe^2+ and S^2− in Overlying Water

Amorphous ferrous sulfide has been identified as a key blackening agent in the occurrence of black water; hence, concentrations of Fe^{2+} and S^{2-} were monitored during the experiments. Initially, $\rho(Fe^{2+})$ of the water was high, because of plentiful cyanobacteria in the water-column. Over time, the algal residue sank gradually to the sediment-surface and $\rho(Fe^{2+})$ of the water declined slightly. During the black-water occurrence and sustaining period, $\rho(Fe^{2+})$ rose to maximum values, decreasing sharply thereafter to a stable concentration [Figure 5]. $\rho(Fe^{2+})$ of all samples with black-water occurrence was always higher than those of the others throughout the experiment ($P < 0.05$). Moreover, $\rho(Fe^{2+})$ of the treatments with a darker black-coloration (PT2, Blank, and CK) was significantly higher than that with a lighter coloration (PT10), and the one with no black-water occurrence (PT15) [$P < 0.05$]. The results indicate that as the black-water system had highly reductive characteristics, the original geochemical balance in the aquatic environment was broken,; Fe^{3+} in the columns was reduced, while Fe^{2+} was partially produced, causing Fe to move toward an Fe^{2+} dominant condition.

In the highly reductive environment, SO_4^{2-} was also reduced. Meanwhile, the anaerobic decomposition of sulfurous amino acids from plankton could also cause an increase in S^{2-} concentrations. Here, the variation tendency of $\rho(S^{2-})$ was similar to that of $\rho(Fe^{2+})$ [Figure 6]. $\rho(S^{2-})$ in PT15 was also lower than that of other samples with black-water occurrence; the former values were 57.1–75.0% of the latter.

PT reversed the positions of polluted surface-sediments and the bottom-sediments with a lack of contaminants, forming a new sediment–water interface. The accumulation of Fe^{2+} and S^{2-} in the overlying water significantly decreased, ultimately inhibiting the production of the key blackening components, viz., amorphous FeS.

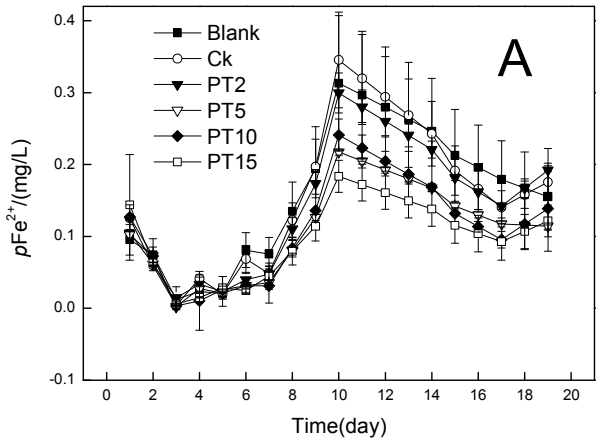

Figure 5. *Concentration of (Fe^{2+}) in overlying water during the black water enents.*

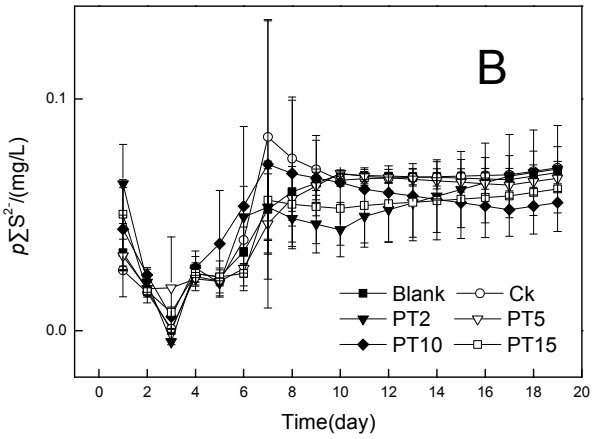

Figure 6. *Concentration of (S^{2-}) in overlying water during the black water enents.*

3.4. Concentrations of Fe^{2+} and S^{2-} in Sediment Interstitial-Water

Fe and S are considered as the key factors influencing black-water events [15-16]. Hence, analyzing the variation of ρ(Fe^{2+}) and ρ(S^{2-}) in sediment interstitial-water could help clarify how PT prevents and controls black-water events in shallow lakes.

ρ(Fe^{2+}) in all samples with black-water occurrence was significantly higher than that of others (PT15) [$P < 0.05$]; the former being 3–4 times that of the latter (Figure 7). ρ(Fe^{2+}) in all samples with black-water occurrence accounted for 40% of ρ(TFe); being only 25% in PT15 (Figure 8), suggesting that the Fe redox system of the sediment-surface was modified by the highly reductive environment, and the existing valence state transformed from Fe(III) to Fe(II) [38]. Ultimately, the accumulation of Fe^{2+} on the sediment-surface provided material basis for water-blackening [10, 15, 39].

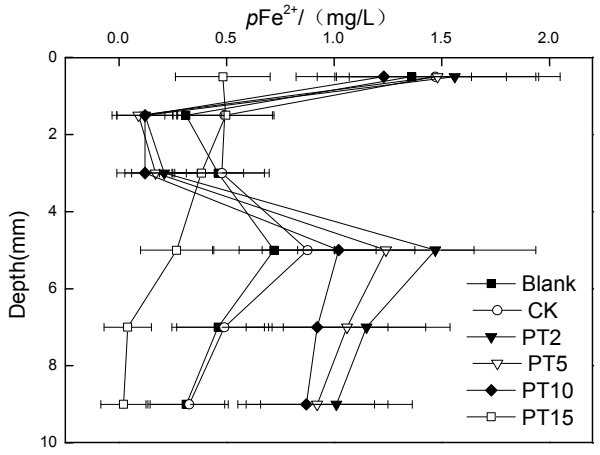

Figure 7. *Profile of Fe^{2+} in pore water after the black water events.*

The existence of AVS in the sediments is considered to be a complex symptom of the production, oxidation, and diffusion of sulfide [40]. Figure 9 shows variations of ω(AVS) (μg/g) in sediment profiles after the experiment; AVS was not detected in PT15. While AVS values in the groups with black-water occurrence were all high ($P < 0.05$), indicating an accumulation of AVS, the values decreased sharply for a while before achieving stability. ω(AVS) generally varied with sediment depth. In the slightly polluted or unpolluted sediments, it tended to have a low concentration on the surface, increasing with depth (up to a maximum of 10–20 cm), then declining gradually with depth [41, 42]. Our results apparently differed from previous studies, probably because of the formation and persistence of an anaerobic reductive environment in the columns, enabling SRB to multiply [43], reducing the sulfur-containing substances ultimately resulting in the storage of AVS.

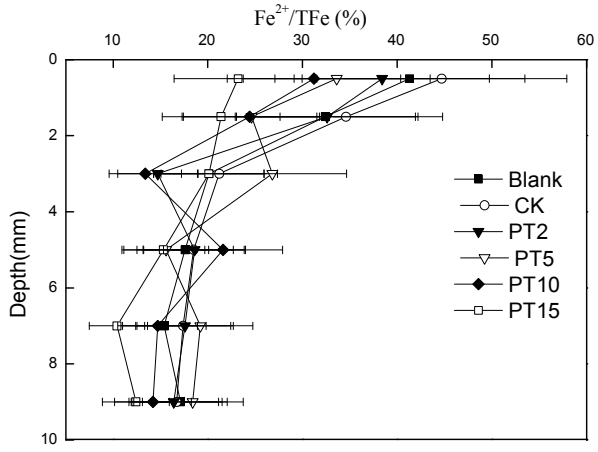

Figure 8. *Profile of percentage of Fe^{2+} to TFe in pore water after the black water events.*

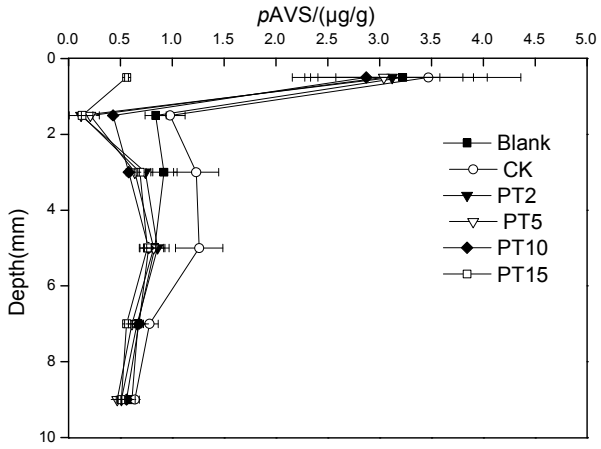

Figure 9. *Profile of AVS in pore water after the black water events.*

4. Conclusions

1) The black-water phenomenon occurred in water-columns of CK, PT2, PT5, and PT10 between days 8–14 successively. E_h was 0 mV in the sediment layer a few millimeters apart from the surface. In this highly reducing surface sediment, the existing valence state of Fe began to transform from Fe(III) to Fe(II); significant amounts of AVS also accumulated, ultimately providing material basis for water-blackening.

2) The black-water phenomenon did not occur in treatment PT15; $\rho(Fe^{2+})$ and $\rho(S^{2-})$ in the overlying water, both considered as key blackening agents, accounted for 46.7–79.5% and 57.1–75.2%, respectively, of the groups with black-water occurrence. $\rho(Fe^{2+})$ in sediment interstitial-water of PT15 was 0.54 mg/L, being 25.3–33.7% of the groups with black-water occurrence. $\rho(Fe^{2+})$ was 25.2% of ρ(TFe), far below that of the groups with black-water occurrence (~40%). ω(AVS) in surface sediments was 0.51 μg/g, accounting for 14.6–17.2% that of the groups with black-water occurrence; both proving that a reasonable PT-depth (>15 cm) can help control the formation of a highly reducing environment due to excessive algae on sediment surface, preventing an over-transformation of Fe(III) to Fe(II), restricting accumulation of AVS caused by excessive growth and reproduction of SRB in surface sediment and ultimately restraining the formation of blackening substances like FeS.
3) As a physical sediment remediation technique, PT was implemented for ecological reconstruction of the surface sediments in algal accumulation areas by relocating polluted surface sediments to deeper layers, which could prevent the formation of blackening substances and ultimately control the black water phenomenon.
4) The deeper the implementation of PT, more evident was its effects on preventing and controlling the black-water phenomenon. However, a deeper PT application also requires more practical measures. In conclusion, maximizing the efficiency of PT instruments at deeper PT-depths needs further research. Additionally, restoration of benthic communities and controlling the release of internal nutrients needs consideration.

Acknowledgements

This work was supported by Key Research and Development Projects of Anhui Province, China (201904a05020053); Housing and Urban-Rural Development Science and Technology Program of Anhui Province, China (No. 2017YF-02); Major Science and Technology Program for Water Pollution Control and Treatment of China (No. 2012ZX07103-005).

References

[1] H. W. Paerl, H. Xu, M. J. Mccarthy, *et al*. "Controlling harmful cyanobacterial blooms in a hyper-eutrophic lake (Lake Taihu, China): the need for a dual nutrient (N & P) management strategy" [J]. Water Research, 2011, 45 (5): 1973-1983.

[2] R. C. Aller. "Bioturbation and remineralization of sedimentary organic matter: effects of redox oscillation" [J]. Chemical Geology, 1994, 114 (3): 331-345.

[3] D. Scavia, N. N. Rabalais, R. E. Turner, et al. "Predicting the response of Gulf of Mexico hypoxia to variations in Mississippi River nitrogen load"[J]. Limnology and Oceanography, 2003, 48 (3): 951-956.

[4] W. M. Kemp, W. R. Boynton, J. E. Adolf, et al. "Eutrophication of Chesapeake Bay: historical trends and ecological interactions" [J]. Marine Ecology Progress Series, 2005, 303: 1-29.

[5] M. Yang, J. W. Yu, Z. L. Li, et al. "Taihu Lake not to blame for Wuxi's woes" [J]. Science, 2008, 319 (5860): 158.

[6] Q. Shen, Q. Zhou, S. Shao, et al. "Estimation of in-situ sediment nutrients release at the submerged plant induced black bloom area in Lake Taihu"[J]. Jounal of Lake Science, 2014, 26 (2): 177-184.

[7] G. Lu and Q. Ma. "Analysis on the causes of forming black water cluster in Taihu Lake" [J]. Advanceds in water science, 2009 (3): 438-442.

[8] G. Lu and Q. Ma. "Monitoring and analysis on "Black Water Aggregation" in Lake Taihu, 2009" [J]. Jounal of Lake Science, 2010 (4): 481-487.

[9] D. Sheng, Z. Xu, Y. Gao. "Cause and impact analysis of black water cluster in Taihu Lake" [J]. Water Resources protection, 2010 (3): 41-44.

[10] G. Liu, J. Zhong, J. He, et al. "Effects of black spots of dead-cyanobacterial mats on Fe-S-P cycling in sediments of Zhushan Bay, Lake Taihu" [J]. Environmental Science. 2009 (9): 2520-2526.

[11] W. He, J. Shang, X. Lu, et al. "Effects of sludge dredging on the prevention and control of algae-caused black bloom in Taihu Lake, China" [J]. Journal of Environmental Sciences, 2013, 25 (3): 430-440.

[12] J. Chen, D. Zhang, J. Song, et al. "Experimental study on restoration of aged beach for culturing Sinonovacula constricta in Rushan Bay" [J]. Marine Fisheries Research, 2005, 5: 57-61.

[13] S. Ma, F. Xin, D. Zhang, J. Song, et al. "Studies on short-necked clam culture in the recovery areas of Rushan Bay" [J]. Marine Fisheries Research, 2005, 2: 59–61.

[14] X. Gu, K. Chen, W. Huang, et al. "Preliminary application of a novel and cost-effective insite technology in compacted lakeshore sediments for wetland restoration" [J]. Ecological Engineering, 2012, 44: 290-297.

[15] Q. Shen, C. Liu, Q. Zhou, et al. "Effects of physical and chemical characteristics of surface sediments in the formation of shallow lake algae-induced black bloom" [J]. Jounal of Environmental Science, 2013, 12: 2353-2360.

[16] C. Liu, Q. Shen, Q. Zhou, et al. "Precontrol of algae-induced black blooms through sediment dredging at appropriate depth in a typical eutrophic shallow lake"[J]. Ecological Engineering, 2015, 77: 139-145.

[17] L. L. Stookey. "Ferrozine: a new spectrophotometric reagent for iron" [J]. Analytical chemistry, 1970, 42 (7): 779-781.

[18] Chineseepa. "Methods for the examination of water and wastewater 4th edition" [M]. 4th. Beijing: China Environmental Science Press, 2002.

[19] E. J. Phillips, D. R. Lovley. "Determination of Fe(III) and Fe(II) in oxalate extracts of sediment" [J]. Soil Science Society of America Journal, 1987, 51 (4): 938-941.

[20] A. D. McQueen, C. M. Kinley-Baird, Kyla Lwinski, A. J. Calomeni. "Effects of Acid Volatile Sulfides (AVS) from Na_2S-amended sediment on Hyalella azteca" [J]. Water Air and Soil Pollution, 2016, 227 (5): 2-10.

[21] Y. Hsieh, Y. Shieh. "Analysis of reduced inorganic sulfur by diffusion methods: improved apparatus and evaluation for sulfur isotopic studies" [J]. Chemical Geology, 1997, 137 (3): 255-261.

[22] G. A. Ulrich, L. R. Krumholz, J. M. Suflita. "A rapid and simple method for estimating sulfate reduction activity and quantifying inorganic sulfides" [J]. Applied and environmental microbiology, 1997, 63 (4): 1627-1630.

[23] M. W. Beutel. "Hypolimnetic anoxia and sediment oxygen demand in California drinking water reservoirs" [J]. Lake and Reservoir Management, 2003, 19 (3): 208-221.

[24] B. B. Jorgensen, R. N. Glud, O. Holby. "Oxygen distribution and bioirrigation in Arctic fjord sediments (Svalbard, Barents Sea)" [J]. Marine Ecology Progress Series, 2005, 292 (3351): 85-95.

[25] R. N. Glud. "Oxygen dynamics of marine sediments" [J]. Marine Biology Research, 2008, 4 (4): 243-289.

[26] K. M. Sherman, B. C. Coull. "The response of meiofauna to sediment disturbance" [J]. Journal of Experimental Marine Biology and Ecology, 1980, 46 (1): 59-71.

[27] D. C. Reicosky, D. W. Archer. "Moldboard plow tillage depth and short-term carbon dioxide release" [J]. Soil and Tillage Research, 2007, 94 (1): 109-121.

[28] E. Duport, F. Gilbert, J. C. Poggiale, et al. "Benthic macrofauna and sediment reworking quantification in contrasted environments in the Thau Lagoon" [J]. Estuarine, Coastal and Shelf Science, 2007, 72 (3): 522-533.

[29] Y. Gao, J. Cornwell, D. Stoecker, et al. "Effects of cyanobacterial-driven pH increases on sediment nutrient fluxes and coupled nitrification-denitrification in a shallow fresh water estuary" [J]. Biogeosciences, 2012, 9 (7): 2697-2710.

[30] W. J. Cai, G. W. Luther, J. C. Conwell, et al. "Carbon cycling and the coupling between proton and electron transfer reactions in aquatic sediments in Lake Champlain" [J]. Aquatic Geochemistry, 2010, 16 (3): 421-446.

[31] M. Chen, T. R. Ye, L. R. Krumholz, et al. "Temperature and cyanobacterial bloom biomass influence phosphorous cycling in eutrophic lake sediments" [J]. PloS one, 2014, 9 (3): e93130.

[32] Z. Feng, C. Fan, W. Huang, et al. Microorganisms and typical organic matter responsible for lacustrine "black bloom"[J]. Science of the Total Environment, 2014, 470–471 (0): 1-8.

[33] S. Gerhardt and B. Schink. "Redox changes of iron caused by erosion, resuspension and sedimentation in littoral sediment of a freshwater lake" [J]. Biogeochemistry, 2005, 74 (3): 341-356.

[34] R. J. Diaz and R. Rosenberg. "Spreading dead zones and consequences for marine ecosystems" [J]. Science, 2008, 321 (5891): 926-929.

[35] B. Duval, S. D. Ludlam. "The Black Water Chemocline of Meromictic Lower Mystic Lake, Massachusetts, U.S.A" [J]. International Review of Hydrobiology, 2001, 86 (2): 165-181.

[36] J. H. Sharp. "Estuarine oxygen dynamics: What can we learn about hypoxia from long-time records in the Delaware Estuary?" [J]. Limnology and Oceanography, 2010, 55 (2): 535.

[37] Q. Shen, Q. Zhou, J. Shang, et al. "Beyond hypoxia: occurrence and characteristics of black blooms due to the decomposition of the submerged plant Potamogeton crispus in a shallow lake" [J]. Journal of Environmental Sciences, 2014, 26 (2): 281-288.

[38] X. Li, X. Lu, Y. Sun, et al. "Relation of active iron and redox environments in the sediments of Bohai Sea" [J]. Marine Environmental Science, 2003, (01): 20-24.

[39] G. Liu, Q. Shen, L. Zhang, et al. "Environment effects of algae-caused black spots: driving effects on the N, P changes in the water-sediment interface" [J]. Environmental Science, 2010, (12): 2917-2924.

[40] D. Rickard, J. W, Morse. "Acid volatile sulfide (AVS)" [J]. Marine Chemistry, 2005, 97 (3): 141-197.

[41] V. Griethuysen, Gillissen F, Koelmans A. "Measuring acid volatile sulphide in floodplain lake sediments: effect of reaction time, sample size and aeration" [J]. Chemosphere, 2002, 47 (4): 395-400.

[42] Fang T, Li X, Zhang G. "Acid volatile sulfide and simultaneously extracted metals in the sediment cores of the Pearl River Estuary, South China" [J]. Ecotoxicology and Environmental Safety, 2005, 61 (3): 420-431.

[43] Feng Z, FAN C, Huang W, et al. Microorganisms and typical organic matter responsible for lacustrine "black bloom" [J]. Science of the Total Environment, 2014, 470: 1–8.